

The coding of valence and identity in the mammalian taste system

Li Wang^{1,2,3}, Sarah Gillis-Smith^{1,2,3}, Yueqing Peng^{1,2,3}, Juen Zhang^{1,2,3}, Xiaoke Chen^{1,2,6}, C. Daniel Salzman^{3,4}, Nicholas J. P. Ryba⁵ & Charles S. Zuker^{1,2,3*}

The ability of the taste system to identify a tastant (what it tastes like) enables animals to recognize and discriminate between the different basic taste qualities^{1,2}. The valence of a tastant (whether it is appetitive or aversive) specifies its hedonic value and elicits the execution of selective behaviours. Here we examine how sweet and bitter are afforded valence versus identity in mice. We show that neurons in the sweet-responsive and bitter-responsive cortex project to topographically distinct areas of the amygdala, with strong segregation of neural projections conveying appetitive versus aversive taste signals. By manipulating selective taste inputs to the amygdala, we show that it is possible to impose positive or negative valence on a neutral water stimulus, and even to reverse the hedonic value of a sweet or bitter tastant. Remarkably, mice with silenced neurons in the amygdala no longer exhibit behaviour that reflects the valence associated with direct stimulation of the taste cortex, or with delivery of sweet and bitter chemicals. Nonetheless, these mice can still identify and discriminate between tastants, just as wild-type controls do. These results help to explain how the taste system generates stereotypic and predetermined attractive and aversive taste behaviours, and support the existence of distinct neural substrates for the discrimination of taste identity and the assignment of valence.

The taste system is responsible for detecting and responding to the five basic taste qualities: sweet, sour, bitter, salty and umami^{1,2}. Each of these five tastes is detected by specialized taste receptor cells on the tongue and palate epithelium, with different taste receptor cells dedicated to each of the taste modalities^{1,2}. In rodents, taste information travels from taste receptor cells in the oral cavity to primary gustatory cortex (insular cortex) via four neural stations^{1,3}: taste receptor cells to taste ganglia, then to the nucleus of the solitary tract, the parabrachial nucleus, the thalamus and to insular cortex. Intrinsic^{4,5} and two-photon⁶ imaging studies have shown that sweet and bitter taste are represented in the cortex in topographically separate cortical fields; by optogenetically activating these taste cortical fields in awake mice, it is possible to evoke prototypical taste behaviours in the total absence of taste stimuli⁷.

The two most important sensory features of a taste stimulus are its identity and its valence. We hypothesized that by examining the neural targets of the sweet and bitter cortical fields it may be possible to uncover the circuit logic for appetitive versus aversive tastes. To trace the projections of neurons in the sweet and bitter cortex, we labelled neurons in the sweet cortical field with enhanced green-fluorescent protein (eGFP), those in the bitter cortex with red-fluorescent protein (tdTomato), and then the whole brains were examined by clearing and rapid 3D imaging with light-sheet microscopy using clear, unobstructed brain imaging and computational analysis (CUBIC)⁸. Our results show that projections from the sweet and bitter cortical fields target multiple brain areas, including contralateral taste cortex, amygdala, entorhinal cortex, caudoputamen and thalamus (see Fig. 1). Notably, sweet and

bitter cortical projections exhibited strong segregation as separate lines while navigating to the amygdala (Fig. 1b, c and Extended Data Fig. 1), with neurons from the sweet cortical field terminating in the anterior basolateral amygdala (BLA), whereas neurons from the bitter cortical field predominantly projected to central amygdala (CEA), with some

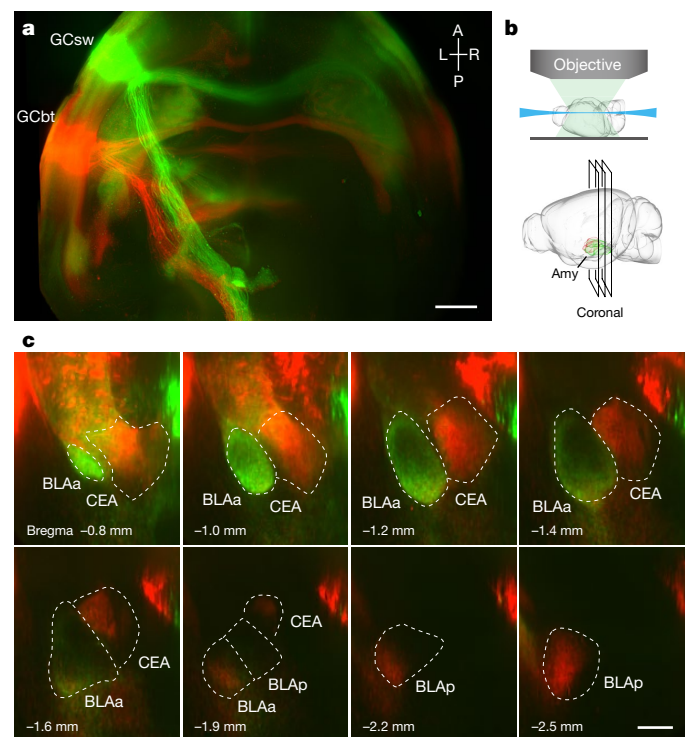


Fig. 1 | Projections from the sweet cortex and the bitter cortex terminate in distinct targets in the amygdala. **a**, Maximum-intensity z stack of projections⁸ from the sweet cortical field labelled with eGFP (GCsw, green) and the bitter cortical field labelled with tdTomato (GCbt, red). A, anterior; P, posterior; L, left; R, right. Scale bar, 1 mm. **b**, Schematic of whole-brain imaging with light-sheet fluorescence microscopy⁸, illustrating the coronal sections shown in **c**. Amy, amygdala. The brain diagrams were rendered by the scalable brain composer (https://scalablebrainatlas.incf.org/services/sba-composer.php?template=ABA_v3) based on Allen Mouse Brain Common Coordinate Framework version 3^{26,27}. **c**, Segregation of sweet and bitter projections. Sweet cortical neurons project to the anterior BLA (BLAa, green), whereas bitter cortical neurons predominantly innervate the CEA (red) and a portion of the posterior BLA (BLAp, red; see also Extended Data Fig. 1). Scale bar, 0.5 mm. The boundaries of amygdala nuclei were based on the Allen Brain Institute atlas²⁶ (<http://brain-map.org/>). Similar results were observed in six animals.

¹Howard Hughes Medical Institute, Columbia University, New York, NY, USA. ²Department of Biochemistry and Molecular Biophysics, Columbia College of Physicians and Surgeons, Columbia University, New York, NY, USA. ³Department of Neuroscience, Columbia College of Physicians and Surgeons, Columbia University, New York, NY, USA. ⁴Department of Psychiatry and New York State Psychiatric Institute, Columbia University, New York, NY, USA. ⁵National Institute of Dental and Craniofacial Research, National Institutes of Health, Bethesda, MD, USA. Present address: ⁶Department of Biology, Stanford University, Stanford, CA, USA. *e-mail: cz2195@columbia.edu

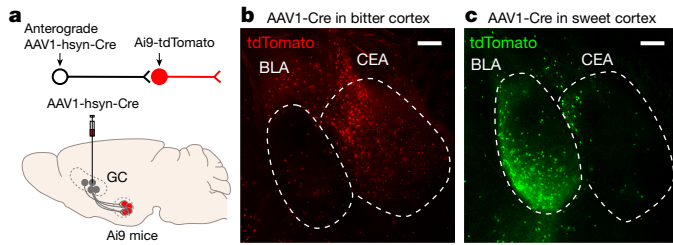


Fig. 2 | Segregation of sweet and bitter targets in the amygdala. **a**, Schematic illustrating anterograde transsynaptic labelling of neurons in the amygdala following AAV1-hsyn-Cre injection⁹ in the sweet or bitter taste cortex of mice expressing a tdTomato reporter. **b, c**, Representative confocal images of tdTomato expression in amygdala following AAV1 injection in the bitter cortex (**b**) or sweet cortex (**c**; pseudocoloured green). Scale bars, 200 μm . Similar results were obtained in three animals for each experiment. See also Extended Data Fig. 2.

terminals in the posterior BLA. We extended these findings by performing anterograde labelling experiments using adeno-associated virus (AAV)-based transsynaptic transfer of Cre-recombinase⁹ from sweet and bitter cortex to targets in the amygdala. These results substantiated that the BLA was the target of sweet cortex projections, and the CEA was the target of bitter cortex projections (Fig. 2; see Extended Data Fig. 2 for activity-dependent labelling).

The amygdala is a key brain structure involved in processing emotions, motivation and positive and negative stimuli^{10–19}. Previous studies have shown that the BLA and CEA both contain distinct populations of neurons that are activated by negative or positive stimuli^{10,13–19}. Our finding of such strong segregation of appetitive (sweet) versus aversive (bitter) projections to the amygdala immediately suggests an anatomical division for the generation of valence-specific behavioural responses to tastants.

If the amygdala imposes valence on tastants (that is, it represents the hedonic value of a tastant to drive valence-specific behaviours), then optogenetic activation of the terminals of sweet cortical neurons in the BLA should elicit attractive responses, whereas activation of bitter projections should evoke aversive behaviours. Therefore, we generated mice expressing channelrhodopsin-2 (ChR2)²⁰ in either the sweet or bitter cortical field, implanted optical fibres over the amygdala, and used a place-preference test to measure responses to photostimulation of the cortico-amygdalar projections. Our results showed that mice avoided the chamber linked to photostimulation of the bitter cortico-amygdalar projections (Extended Data Fig. 3), but exhibited a strong preference for the chamber associated with stimulation of the sweet projections.

Next, we reasoned that optogenetic activation of the terminals of sweet cortical neurons in the BLA would trigger appetitive taste behaviours, whereas stimulation of the projections from bitter cortical neurons in the CEA would instead impose a negative valence on the stimulus. Therefore, we assayed whether ChR2 activation of sweet-to-BLA projections while a mouse is drinking a neutral stimulus (for example, water) transforms it into a highly attractive one such as sugar, and conversely, whether activation of the projections from bitter cortex to CEA trigger strong laser-dependent suppression of licking, much like the introduction of a bitter chemical would do.

We used a behavioural paradigm in which ChR2-expressing mice were assayed for water drinking in a head-restrained setup⁷. In these experiments, the laser shutter was placed under lick-contact operation, and thus the mouse has control of its own stimulation during the light-on trials, and only self-stimulation would continue to trigger appetitive responses (light stimulation on its own does not trigger licking, or licking-like motor responses; see Methods)⁷. By contrast, a mouse would immediately terminate licking if contact-licking elicited aversion. Indeed, optogenetic activation of the sweet cortex terminals in BLA evoked a marked increase in licking (self-stimulation; Fig. 3b, c), whereas activation of the bitter cortical projections to amygdala

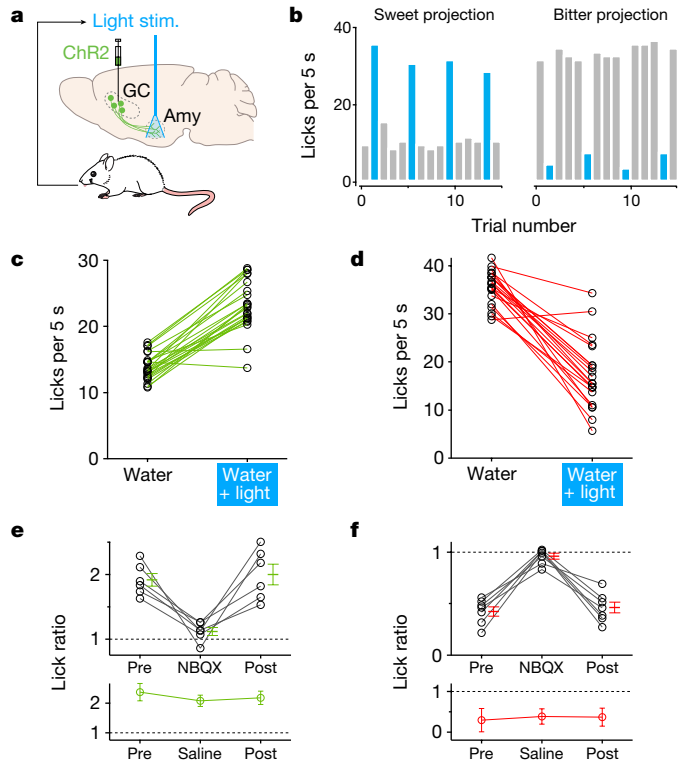


Fig. 3 | Activation of sweet and bitter cortical terminals in the amygdala drives appetitive and aversive behaviours. **a**, Optogenetic stimulation strategy. Sweet neurons in the anterior gustatory cortex (GC) or bitter neurons in posterior gustatory cortex were transduced with AAV-ChR2. Stimulating optical fibres were placed above BLA or CEA. For coupling the photostimulation to drinking behaviour, laser pulses were triggered by licking. **b**, Representative histograms showing licking events in the presence (blue) or absence (grey) of photostimulation of sweet cortico-amygdalar projections (left) or bitter cortico-amygdalar projections (right). Note the marked enhancement or suppression of licking, respectively. **c, d**, Quantification of licking responses with and without light stimulation. **c**, Sweet cortical terminals in the BLA. $n = 24$ mice, two-tailed paired t -test, $P < 0.0001$. **d**, Bitter cortical terminals in the CEA. $n = 21$ mice, two-tailed paired t -test, $P < 0.0001$. See also Extended Data Fig. 4. **e, f**, Pharmacological silencing demonstrated that the light-dependent licking behaviours are due to activity in the amygdala; the panels show quantification of lick ratios before and after infusion of NBQX (top) or control saline (bottom) in the amygdala. **e**, Stimulation of sweet projections. $n = 6$ mice. **f**, Stimulation of bitter projections. $n = 7$ mice. Note that NBQX abolishes the light-dependent changes in licking responses. Values are mean \pm s.e.m. Repeated-measures one-way analysis of variance (ANOVA) followed by Bonferroni post hoc test (Supplementary Table 1).

strongly suppressed licking responses (Fig. 3b, d). To confirm that these light-triggered behaviours were not caused by back-propagation of action potentials from the stimulation in the amygdala (that is, back to the taste cortex and thus to other potential taste cortical targets), we repeated the experiment, however, this time we pharmacologically silenced synaptic activity locally in the amygdala by infusion of the AMPA (α -amino-3-hydroxy-5-methyl-4-isoxazolepropionic acid) receptor antagonist NBQX²¹. Our results demonstrate that silencing synaptic transmission in the amygdala abolished all light-evoked responses (Fig. 3e, f). As expected, responses fully recovered after wash-out of the drug (Fig. 3e, f). Taken together, these data demonstrate that activation of sweet or bitter cortico-amygdalar pathways is sufficient to impose a positive or a negative valence on a neutral taste cue.

We hypothesized that strong activation of the bitter and sweet cortico-amygdalar projections might override the hedonic response elicited by sweet and bitter tastants. Therefore, we predicted that optogenetic activation of the bitter cortical terminals in the CEA may impose an

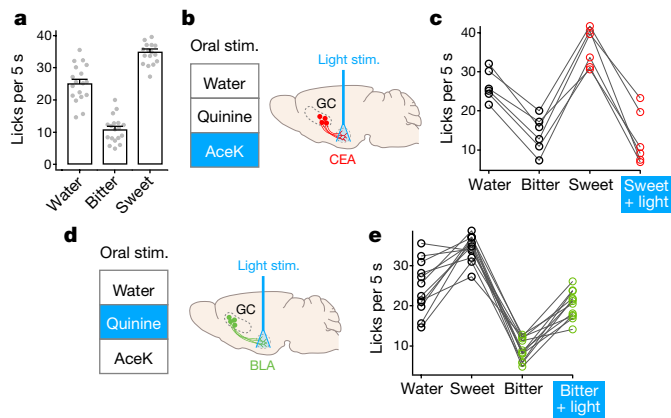


Fig. 4 | Activation of cortico-amygdalar circuits overrides the hedonic valence of orally delivered tastants. **a**, Licking responses (no photostimulation) to water, bitter (0.5 mM quinine) and sweet (4 mM AceK) stimuli. $n = 18$ mice; data are mean \pm s.e.m. **b**, Schematic of optogenetic stimulation strategy; AAV-ChR2 was injected into the bitter cortex and the optical fibre was placed above the CEA. **c**, Quantification of licking response to water, bitter and sweet stimuli and sweet stimuli plus light. $n = 6$ mice. Stimulation overrides the attractive responses to the sweet stimulus. **d**, Schematic of photostimulation of sweet terminals. **e**, Quantification of licking response to water, sweet and bitter stimuli and bitter stimuli plus light. $n = 12$ mice. Stimulation overrides the aversive responses to the bitter stimulus. Repeated-measures one-way ANOVA followed by Bonferroni post hoc test; see Supplementary Table 1.

aversive response to an orally applied sweet tastant, whereas strong stimulation of sweet terminals in BLA might suppress aversion to an orally applied bitter tastant. We used a behavioural test in which thirsty mice expressing ChR2 in the bitter or sweet cortex were exposed to random presentations of water, a bitter chemical or a sweet solution (Fig. 4a). Next, we examined the effect of photoactivating bitter cortico-amygdalar projections by placing the stimulating optical fibre over the amygdala of mice that expressed ChR2 in the bitter cortex (Fig. 4b). Stimulation of bitter targets in the amygdala is indeed sufficient to transform the appetitive nature of a sweet tastant into an aversive one (Fig. 4c). Conversely, by photoactivating the amygdala targets of the sweet cortex it was possible to change the perceived valence of a bitter tastant (Fig. 4d, e). These results highlight the key role of the amygdala in imposing valence on a taste cue. To examine the effect of taste stimulation in the absence of amygdala function, we carried out a number of studies in which the neurons of the amygdala were reversibly silenced.

First, we used a behavioural assay that relies on direct stimulation of the taste cortex. In one group of mice, we introduced ChR2 into neurons in the sweet cortical field (Fig. 5a), bilaterally injected an AAV encoding inhibitory designer receptors exclusively activated by designer drugs (DREADD) into amygdala neurons for chemogenetic silencing²² (see Methods for details), and tested the mice before and after clozapine *N*-oxide (CNO) injection. Importantly, ChR2 and the stimulating fibre are both in the sweet cortex (Fig. 5a), and because sweet neurons project to many targets (see Fig. 1a), the full repertoire is likely to be co-activated upon stimulation of the sweet cortical field. Notably, silencing of the amygdala was sufficient to abolish all attractive responses associated with activation of the sweet cortex (Fig. 5b); equivalent results were obtained using pharmacological inhibition of the amygdala with NBQX rather than inhibitory DREADD (Fig. 5c). We repeated similar studies but this time examined the activation of the bitter cortex (Fig. 5d). Our results showed that silencing of the amygdala is also sufficient to abolish aversive responses associated with the activation of the bitter cortex (Fig. 5e, f). Finally, we reasoned that the valence associated with sweet and bitter tastants delivered to the tongue, rather than direct stimulation of the taste cortex, could also be compromised. As predicted, the results shown in Fig. 5g–i demonstrate that silencing the amygdala impairs the behavioural preference for sweet chemicals and the aversion to bitter chemicals.

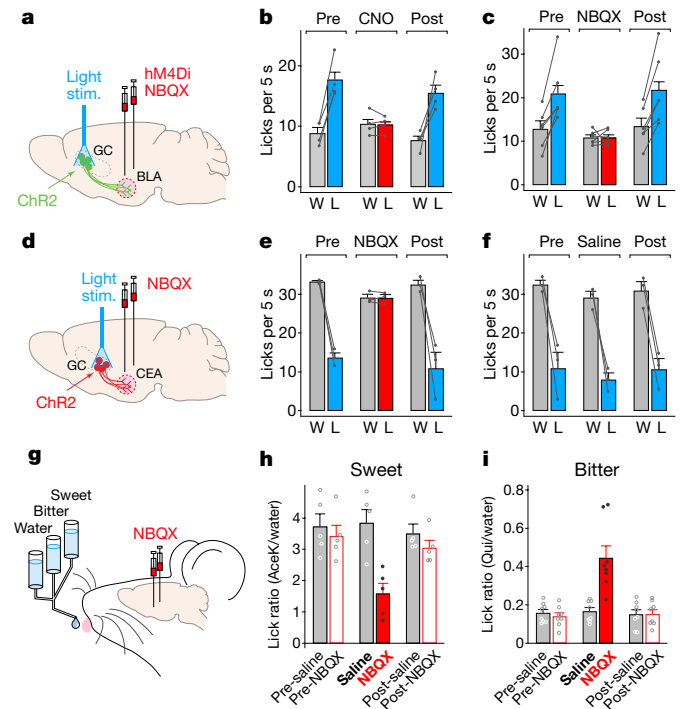


Fig. 5 | Silencing neurons in the amygdala impairs taste valence.

a, Schematic of optogenetic stimulation and the chemogenetic/pharmacological silencing strategy. AAV-ChR2 was injected unilaterally into the sweet cortex, and an optical fibre was implanted for photostimulation. AAV-hM4Di²⁸ was targeted bilaterally to the BLA for chemogenetic silencing (alternatively, cannulas were implanted bilaterally over the amygdala for pharmacological silencing). **b**, Chemogenetic silencing of the amygdala with inhibitory DREADD (hM4Di) and CNO abolished the strong appetitive behaviour observed following photostimulation of sweet cortex (compare pre and post with CNO). $n = 4$ mice, water (W) versus water plus light (L), two-tailed paired *t*-test; pre, $P = 0.0054$; CNO, $P = 0.8900$; post, $P = 0.0265$. See Extended Data Fig. 5 for controls. **c**, Pharmacological silencing of the amygdala with NBQX similarly abolished the appetitive behaviour associated with photostimulation of the sweet cortex. $n = 6$ mice, two-tailed paired *t*-test; pre, $P = 0.0049$; NBQX, $P = 0.9458$; post, $P = 0.0042$. See Extended Data Fig. 5 for controls. **d**, **e**, NBQX silencing of the amygdala abolished aversive responses to photostimulation of the bitter cortex. $n = 3$ mice, two-tailed paired *t*-test; pre, $P = 0.0047$; NBQX, $P = 0.9125$; post, $P = 0.0261$. **f**, Saline controls for NBQX silencing following photostimulation of the bitter cortex. $n = 3$ mice, two-tailed paired *t*-test; pre, $P = 0.0261$; saline, $P = 0.0230$; post, $P = 0.0005$. **g–i**, NBQX silencing of the amygdala diminished preference for sweet chemicals ($n = 5$ mice) and aversion to bitter chemicals ($n = 8$ mice); the small remaining responses to the orally applied sweet and bitter tastants probably reflect brain-stem-dependent immediate reactions to taste observed in decerebrated animals²⁹. Repeated-measures one-way ANOVA followed by Bonferroni post hoc test (Supplementary Table 1). Values are mean \pm s.e.m.

Previously, we showed that silencing the sweet or bitter cortex prevented the recognition of sweet or bitter tastants, whereas optogenetic activation of those same cortical fields triggered prototypical sweet- and bitter-associated behaviours⁷. We reasoned that if tastant identity and valence are encoded in separate neural substrates, with the taste cortex responsible for imposing identity to a tastant, and the amygdala for affording its valence, then mice with silenced amygdala should still recognize the identity of a sweet or bitter taste stimulus, even if blind to its hedonic value.

We trained mice to report the identity of a tastant by using two different behavioural assays: a three-port test and a go/no-go assay. In the three-port test, mice learned to sample a taste cue from a centre spout (random presentations of water, a sweet or a bitter chemical), and then report its identity either by going to the right or left port;

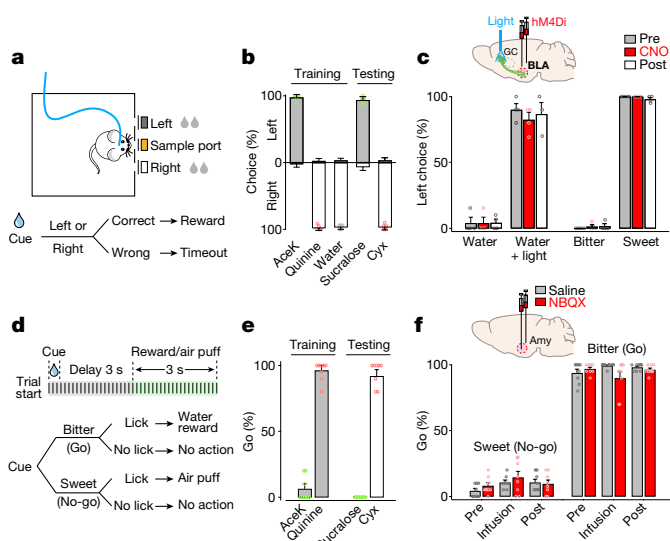


Fig. 6 | Silencing the amygdala does not prevent tastant recognition. **a**, Schematic and flow chart for the three-port taste-recognition task. In each trial, a mouse had 0.5 s to lick a randomly presented taste cue from the middle port, and then go to either the left or right to report the identity of the tastant (in this example mice were trained to go left for sweet and right for bitter or water); correct responses were rewarded with 4 s of water, whereas incorrect ones led to a 5-s timeout penalty. **b**, Quantification of results from three-port recognition sessions, demonstrating highly reliable recognition of the stimulus identity (>90% accuracy). $n = 6$ mice. Tastant concentrations: 10 mM AceK, 1 mM quinine, 3 mM sucralose, 10 μ M cycloheximide (Cyx). **c**, The mice used in Fig. 5b were assayed for the effect of silencing the amygdala. $n = 4$ mice for pre, CNO; $n = 3$ mice for post. Mice with a silenced amygdala can still identify the different tastes with normal accuracy. Importantly, photostimulation of the sweet cortex is recognized as a sweet-tasting stimulus⁷, and remains so after CNO silencing of the amygdala (compare water with water plus light). The graph only presents the responses to the left port (sweet identity). **d**, The animals used in Fig. 5e, h, i were assayed using go/no-go tastant recognition tests⁷. **e**, Mice show highly reliable recognition of the stimulus identity after training (>90% accuracy). $n = 8$ mice. Tastant concentrations: 4 mM AceK, 1 mM quinine, 3 mM sucralose, 10 μ M Cyx. **f**, Pharmacological silencing of amygdala has no significant effect on either sweet or bitter recognition. $n = 8$ mice. Two-way or repeated-measures one-way ANOVA followed by Bonferroni post hoc test (Supplementary Table 1). Values are mean \pm s.e.m.

a correct response was rewarded with 4 s of water (Fig. 6a). We initially focused on attractive responses as they represent the expression of a selective, positive behavioural response. After 20–30 sessions of training over 10–14 days (see Methods for details), trained mice were able to report the identity of each tastant in hundreds of randomized trials with over 90% accuracy (see Fig. 6b), showed correct behavioural responses to other sweet and bitter tastants that were not used in the training set (Fig. 6b, compare training to testing), and appropriately reported direct optogenetic activation of the sweet taste cortex as sweet, with approximately 90% of the water plus light trials producing correct responses (Fig. 6c, pre-silencing). Next, we assayed whether silencing of the amygdala using inhibitory DREADD in the BLA affected the ability of these mice to correctly identify a sweet stimulus. Our results (Fig. 6c) demonstrated that loss of amygdala function, while abolishing the ability of the sweet cortex to evoke appetitive responses (Fig. 5a–c), has no impact on the ability of the mice to properly identify sweet tastants (or to recognize light activation of the sweet cortex as sweet). As anticipated, inhibitory DREADD expression in the sweet cortex (just as has previously been shown using NBQX⁷), severely impairs sweet taste recognition (Extended Data Fig. 6).

The second behavioural platform relied on go/no-go behavioural assays, and examined both sweet and bitter recognition. Thirsty mice were trained to sample a test tastant from a spout, and then to report its

identity either by licking (go) or withholding licking (no-go; Fig. 6d). We trained animals to report ‘go’ when tasting bitter tastants and ‘no-go’ in response to sweet tastants, exactly the opposite of the innate drive. After 15–20 sessions of training, mice reported tastant identity with over 90% accuracy (Fig. 6e). Indeed, silencing of the amygdala, just as observed in the three-port tests, has no effect on recognition of sweet or bitter tastants (Fig. 6f). Notably, these experiments used the same mice that exhibited loss of sweet and bitter valence after NBQX infusion into the amygdala (Fig. 5). Taken together, these studies show that the amygdala is necessary and sufficient to drive valence-specific behaviours to taste stimuli and that the cortex can independently represent taste identity.

The senses of taste and smell function as the principal gateways for assessing the attraction to, and palatability of, food cues. In its most fundamental state, taste mediates innate consummatory and rejection behaviours, while also allowing an animal to learn the association of food sources with hardwired tastant-dependent actions. Here we studied the neural basis for innate responses to sweet and bitter, and showed that the taste cortex and the amygdala function as two essential, but distinct, neural stations for identifying tastants and for imposing valence on sweet and bitter.

Recent molecular studies have identified distinct populations of neurons in the amygdala that may serve as neural substrates for a wide range of positive and negative hedonic responses^{10,13–19}. In this study, we show that sweet and bitter cortical fields exhibit separate projection targets in the amygdala, and that photoactivation of these cortico-amygdalar projections evokes opposing responses. However, these can be experimentally dissociated from the cortex, such that animals may recognize a ‘taste stimulus’ but remain oblivious to its valence. Together, these results provide an anatomical substrate for imposing hedonic value to sweet and bitter, and the basic logic for the generation of hardwired, stereotypic attractive and aversive taste responses.

The amygdala is known to provide representations of Pavlovian associations^{11,23,24}, such that innately rewarding and aversive tastants may also function as unconditioned stimuli in conditioning protocols²⁵. Therefore, in addition to imposing valence on tastants, the amygdala probably links taste valence to other stimuli so that associative memories can be formed, and thereby appropriate valence-specific behaviour may be elicited by previously neutral cues from other modalities that would now predict a bitter or sweet tastant. Notably, the sweet and bitter cortex project to several additional brain areas, including those involved in feeding, motor systems, multisensory integration, learning and memory (Fig. 1). In the future, it will be exciting to unravel how these circuits come together to drive innate and learned responses.

Online content

Any Methods, including any statements of data availability and Nature Research reporting summaries, along with any additional references and Source Data files, are available in the online version of the paper at <https://doi.org/10.1038/s41586-018-0165-4>.

Received: 3 October 2017; Accepted: 26 March 2018;

Published online: 30 May 2018

- Yarmolinsky, D. A., Zuker, C. S. & Ryba, N. J. Common sense about taste: from mammals to insects. *Cell* **139**, 234–244 (2009).
- Scott, K. Taste recognition: food for thought. *Neuron* **48**, 455–464 (2005).
- Spector, A. C. & Travers, S. P. The representation of taste quality in the mammalian nervous system. *Behav. Cogn. Neurosci. Rev.* **4**, 143–191 (2005).
- Accolla, R., Bathellier, B., Petersen, C. C. & Carleton, A. Differential spatial representation of taste modalities in the rat gustatory cortex. *J. Neurosci.* **27**, 1396–1404 (2007).
- Yoshimura, H., Sugai, T., Fukuda, M., Segami, N. & Onoda, N. Cortical spatial aspects of optical intrinsic signals in response to sucrose and NaCl stimuli. *Neuroreport* **15**, 17–20 (2004).
- Chen, X., Gabitto, M., Peng, Y., Ryba, N. J. & Zuker, C. S. A gustotopic map of taste qualities in the mammalian brain. *Science* **333**, 1262–1266 (2011).
- Peng, Y. et al. Sweet and bitter taste in the brain of awake behaving animals. *Nature* **527**, 512–515 (2015).
- Susaki, E. A. et al. Whole-brain imaging with single-cell resolution using chemical cocktails and computational analysis. *Cell* **157**, 726–739 (2014).

9. Zingg, B. et al. AAV-mediated anterograde transsynaptic tagging: mapping corticocollicular input-defined neural pathways for defense behaviors. *Neuron* **93**, 33–47 (2017).
 10. Cai, H., Haubensak, W., Anthony, T. E. & Anderson, D. J. Central amygdala PKC- δ neurons mediate the influence of multiple anorexigenic signals. *Nat. Neurosci.* **17**, 1240–1248 (2014).
 11. Janak, P. H. & Tye, K. M. From circuits to behaviour in the amygdala. *Nature* **517**, 284–292 (2015).
 12. Paton, J. J., Belova, M. A., Morrison, S. E. & Salzman, C. D. The primate amygdala represents the positive and negative value of visual stimuli during learning. *Nature* **439**, 865–870 (2006).
 13. Douglass, A. M. et al. Central amygdala circuits modulate food consumption through a positive-valence mechanism. *Nat. Neurosci.* **20**, 1384–1394 (2017).
 14. Kim, J., Pignatelli, M., Xu, S., Itohara, S. & Tonegawa, S. Antagonistic negative and positive neurons of the basolateral amygdala. *Nat. Neurosci.* **19**, 1636–1646 (2016).
 15. Namburi, P. et al. A circuit mechanism for differentiating positive and negative associations. *Nature* **520**, 675–678 (2015).
 16. Gore, F. et al. Neural representations of unconditioned stimuli in basolateral amygdala mediate innate and learned responses. *Cell* **162**, 134–145 (2015).
 17. Han, W. et al. Integrated control of predatory hunting by the central nucleus of the amygdala. *Cell* **168**, 311–324 (2017).
 18. Kim, J., Zhang, X., Muralidhar, S., LeBlanc, S. A. & Tonegawa, S. Basolateral to central amygdala neural circuits for appetitive behaviors. *Neuron* **93**, 1464–1479 (2017).
 19. Beyeler, A. C. et al. Organization of valence-encoding and projection-defined neurons in the basolateral amygdala. *Cell Rep.* **22**, 905–918 (2018).
 20. Boyden, E. S., Zhang, F., Bamberg, E., Nagel, G. & Deisseroth, K. Millisecond-timescale, genetically targeted optical control of neural activity. *Nat. Neurosci.* **8**, 1263–1268 (2005).
 21. Tye, K. M. et al. Amygdala circuitry mediating reversible and bidirectional control of anxiety. *Nature* **471**, 358–362 (2011).
 22. Stachniak, T. J., Ghosh, A. & Sternson, S. M. Chemogenetic synaptic silencing of neural circuits localizes a hypothalamus→midbrain pathway for feeding behavior. *Neuron* **82**, 797–808 (2014).
 23. Maren, S. Neurobiology of Pavlovian fear conditioning. *Annu. Rev. Neurosci.* **24**, 897–931 (2001).
 24. Cardinal, R. N., Parkinson, J. A., Hall, J. & Everitt, B. J. Emotion and motivation: the role of the amygdala, ventral striatum, and prefrontal cortex. *Neurosci. Biobehav. Rev.* **26**, 321–352 (2002).
 25. Schoenbaum, G., Chiba, A. A. & Gallagher, M. Neural encoding in orbitofrontal cortex and basolateral amygdala during olfactory discrimination learning. *J. Neurosci.* **19**, 1876–1884 (1999).
 26. Lein, E. S. et al. Genome-wide atlas of gene expression in the adult mouse brain. *Nature* **445**, 168–176 (2007).
 27. Bakker, R., Tiesinga, P. & Kötter, R. The scalable brain atlas: instant web-based access to public brain atlases and related content. *Neuroinformatics* **13**, 353–366 (2015).
 28. Armbruster, B. N., Li, X., Pausch, M. H., Herlitze, S. & Roth, B. L. Evolving the lock to fit the key to create a family of G protein-coupled receptors potentially activated by an inert ligand. *Proc. Natl Acad. Sci. USA* **104**, 5163–5168 (2007).
 29. Grill, H. J. & Norgren, R. The taste reactivity test. II. Mimetic responses to gustatory stimuli in chronic thalamic and chronic decerebrate rats. *Brain Res.* **143**, 281–297 (1978).
- Acknowledgements** We thank M. Tessier-Lavigne, N. Renier and P. Ariel for help with CUBIC; members of the Zuker laboratory and R. Axel for helpful discussions. We also acknowledge the Bio-Imaging Resource Center at Rockefeller University. Research reported in this publication was supported by the National Institute on Drug Abuse of the National Institutes of Health under award number R01DA035025 (C.S.Z.). N.J.P.R. is supported by the Intramural Research Program of the NIH, NIDCR; and C.D.S. was supported by R01 MH082017 from NIMH. C.S.Z. is an investigator of the Howard Hughes Medical Institute and a Senior Fellow at Janelia Farm Research Campus.
- Reviewer information** *Nature* thanks I. de Araujo and P. Kenny for their contribution to the peer review of this work.
- Author contributions** L.W. and S.G.-S. designed the study, carried out the experiments and analysed data. Y.P. and J.Z. performed behavioural experiments. C.S.Z., X.C., N.J.P.R. and C.D.S. designed the study and analysed data. C.S.Z., L.W. and N.J.P.R. wrote the paper.
- Competing interests** The authors declare no competing interests.
- Additional information**
- Extended data** is available for this paper at <https://doi.org/10.1038/s41586-018-0165-4>.
- Supplementary information** is available for this paper at <https://doi.org/10.1038/s41586-018-0165-4>.
- Reprints and permissions information** is available at <http://www.nature.com/reprints>.
- Correspondence and requests for materials** should be addressed to C.S.Z.
- Publisher's note:** Springer Nature remains neutral with regard to jurisdictional claims in published maps and institutional affiliations.

METHODS

Animals and surgery procedures. All procedures were carried out in accordance with the US National Institutes of Health (NIH) guidelines for the care and use of laboratory animals, and were approved by the Columbia University Institutional Animal Care and Use Committee. Seven- to nine-week-old male C57BL/6J mice and B6.Cg-Gt(ROSA)^{tm9(CAG-tdTomato)}Hze/J mice (Ai9)³⁰ were used for viral injections.

Animals were anaesthetized with ketamine and xylazine (100 mg kg⁻¹ and 10 mg kg⁻¹, intraperitoneal), placed into a stereotaxic frame with a close-loop heating system to maintain body temperature, and unilaterally injected with 20–50 nl of AAV carrying ChR2 (AAV9-CamKIIa-hChR2(H134R)-EYFP-WPRE-SV40, Penn Vector Core) either in the sweet cortical field (bregma 1.7 mm; lateral 3.1 mm; ventral 1.8 mm) or the bitter cortical field (bregma -0.35 mm; lateral 4.2 mm; ventral 2.7 mm). The location of the taste cortex was verified by anatomical and optogenetic assays. Anterograde tracing⁶ and retrograde tracing (Extended Data Fig. 7) showed that these cortical areas receive input from the taste thalamus (VPMpc). Photostimulation of these sweet and bitter cortical fields evokes prototypical attractive and aversive taste behaviours, respectively⁷. We also examined behavioural data from 14 ChR2 injections in the middle (Extended Data Fig. 8); six of the animals showed a modest increase in lick responses, 3 exhibited no change and 5 showed a small range of aversion. We believe this variability probably reflects the spread of the injection site.

Following viral injections, a customized implantable fibre (core diameter 200 µm, NA 0.39) was implanted 300–500 µm above the injection site, and guide cannulas (26 gauge, PlasticsOne) were unilaterally or bilaterally implanted above the anterior BLA (bregma -1.0 mm; lateral 3.2 mm; ventral 3.7 mm) or CEA (bregma -1.2 mm; lateral 3.0 mm; ventral 3.7 mm). These guide cannulas were used both for photostimulation of cortical projections and intracranial infusion in pharmacological silencing experiments. A metal head post was attached for head fixation during behavioural tests. All implants were secured onto the skull with dental cement (Lang Dental Manufacturing). For chemo-genetic silencing experiments, 150–250 nl of AAV carrying hM4Di (AAV8-hSyn-hM4Di-mCherry, UNC Vector Core) was injected bilaterally into the BLA (bregma -1.0 mm; lateral 3.2 mm; ventral 4.2 mm) or sweet cortical field (bregma 1.7 mm; lateral 3.1 mm; ventral 1.8 mm) at a slow rate (15 nl min⁻¹). All ventral coordinates listed above are relative to the pial surface. Mice were allowed to recover for at least 2–3 weeks before the start of behavioural experiments. For anterograde transsynaptic tracing, AAV1-hSyn-Cre⁹ (20–50 nl) was injected into the sweet or bitter cortical field of mice carrying a Cre-dependent tdTomato reporter (Ai9³⁰). Mice were examined four weeks after the injection. Placements of viral injections, guide cannulas and implanted fibres were histologically verified at the termination of the experiments using DAPI (1:5,000, Thermo Fisher Scientific) or TO-PRO-3 (1:1,000, Thermo Fisher Scientific) staining of 100-µm coronal sections. A confocal microscope (FV1000, Olympus) was used for fluorescence imaging.

Whole-brain clearing and imaging. For whole-brain tracing of the projections of cortical neurons, we unilaterally injected a small volume (10–20 nl) of mixed AAVs carrying Cre-recombinase and Cre-dependent eGFP (AAV1-CamKII0.4-Cre-SV40 and AAV1-CAG-Flex-eGFP-WPRE-bGH, 1:100, Penn Vector Core) in the sweet cortical field, and the same volume of mixed AAVs carrying Cre-recombinase and Cre-dependent tdTomato (AAV1-CamKII0.4-Cre-SV40 and AAV9-CAG-Flex-tdTomato-WPRE-bGH, 1:100, Penn Vector Core) in the bitter cortical field. Four weeks after AAV injection, mice were transcardially perfused with 5–10 ml of phosphate-buffered saline (PBS) containing 10 U ml⁻¹ heparin, followed by 20 ml 4% paraformaldehyde; brains were post-fixed in 4% paraformaldehyde for an additional 3 h at room temperature. Whole brains were then treated following the CUBIC clearing protocol^{8,31}. To prevent sample deformation caused by temperature fluctuation and to minimize fluorescence loss during clearing, all clearing procedures were performed at room temperature. CUBIC clearing reagents were prepared as previously described^{8,31}. Reagent 1 contained 25 wt% urea (Sigma-Aldrich), 25 wt% N,N,N',N'-tetrakis(2-hydroxypropyl)ethylenediamine (Sigma-Aldrich) and 15 wt% Triton X-100 (Nacal Tesque). Reagent 2 contained 50 wt% sucrose (Sigma-Aldrich), 25 wt% urea, 10 wt% triethanolamine (Sigma-Aldrich) and 0.1% (v/v) Triton X-100. The fixed brains were washed three times with PBS, immersed in reagent 1 (diluted 1:2 in water) overnight with gentle shaking and then incubated in reagent 1 for 7–10 days with gentle shaking. Brains were washed with PBS, degassed in PBS overnight and were then transferred into 5 ml of reagent 2 diluted 1:2 in PBS for 6–24 h before immersion in reagent 2 for 3–7 days for further clearing and reflection index matching. TO-PRO-3 (1:5,000, Thermo Fisher Scientific) was added to reagent 2 for counterstaining. During the immersion in reagent 2, tubes were not shaken to avoid bubbles. Samples were kept in reagent 2 for up to one week at room temperature before imaging.

On the day of imaging, samples were gently wiped to remove reagent 2 residue and transferred into an oil mix (mineral oil and silicone oil 1:1, final refraction index 1.48–1.49) at least 1 h before imaging. Light-sheet fluorescence microscopy

(UltraMicroscope, LaVision BioTec) with a 2× objective lens (0.5 NA, working distance 10 mm) or 4× objective lens (0.3 NA, working distance 6 mm) was used for rapid image acquisition of the whole brain. The samples were sequentially illuminated with a unidirectional light sheet produced by 488-nm, 561-nm and 640-nm lasers and scanned with a z-step size of 8.13–13 µm from ventral to dorsal. Exposure time was 50–200 ms per channel per z step. To cover the whole brain, each sample was imaged either via 4 × 4 tile scans with the 4× lens or using multi-position scans with the 2× lens (three manually assigned positions to cover two hemispheres and brainstem).

Whole-brain image tiles were scaled to 1/8 of the original size and stitched in three dimensions using ImageJ 1.51n (Fiji distribution). The 640-nm channel of the whole-brain data was registered to a reference atlas (Allen Brain Institute, 25-µm resolution volumetric data with annotation map, <http://www.brain-map.org>) using ANTs (advanced normalization tools 1.9.x) with affine transformation^{26,32}. The same transformation was applied to the other two channels using the WarpImageMultiTransform function of ANTs. z projections of maximum intensity and virtual sections were processed in ImageJ (noise was filtered with the remove outlier function). Because of the high dynamic range of the fluorescent intensity between the soma and the fine processes, the gamma value of the images shown in Fig. 1 was set to 0.5 for display purposes.

Fos induction and immunohistochemistry. Mice expressing ChR2 in the sweet or bitter cortex were habituated by performing mock stimulations (see below) once a day for three days before Fos induction. On the day of the experiment, mice were photostimulated for 30 min (473 nm, 20 Hz, 20-ms pulses, 5 s on and 5 s off, 5–10 mW per mm²). Mice were then allowed to rest for 1 h and were processed for immunostaining as previously described⁷. Tissue sections were incubated with goat anti-Fos antibody (1:500, Santa Cruz, sc-52-G) for 24 h at 4°C. Fluorescently tagged secondary antibodies (Alexa-594 donkey anti-goat or Alexa-647 donkey anti-goat, 1:1,000, Thermo Fisher Scientific) were used to visualize Fos expression. All sections were imaged using an Olympus FV-1000 confocal microscope.

Head-restrained lick preference assays. Head-restrained lick preference assays were performed as previously described⁷. Mice expressing ChR2 in the sweet or bitter cortex were initially water-deprived for 24 h to motivate drinking in head-restrained assays and then acclimated to drinking from a motor-positioned spout (two sessions per day for at least two days) before testing. Mice were weighed daily during the behavioural assays and supplied with necessary water to maintain at least 85% of their initial body weight. Each trial began with a light cue, followed 1 s later by the spout swinging into position and a tone cue to indicate the onset of tastant delivery; after 5 s (during which the mouse could lick) the spout rotated out of position. To measure attractive responses, mice were mildly water restricted (water-deprived for 24 h, and then provided with water until they exhibited an average of 5–15 licks per 5-s window); mice were supplied with 2–5 µl water at the beginning of each trial. To measure aversion, mice were water-deprived for 24 h, and supplied with 5–10 µl water per lick; mice normally exhibited active licking over the full five seconds (average 30–40 licks per 5 s as a sign of thirst). Training sessions consisted of 60 trials with water; testing sessions shown in Fig. 3 consisted of 15 trials with water, 4 of which were coupled to photostimulation of cortical terminals in the amygdala; testing sessions in Fig. 5b–f consisted of 20 trials with water, 10 of which were pseudo-randomly coupled to photostimulation of the sweet cortex; testing sessions in Fig. 4 consisted of 60 trials, 20 trials with water, 20 trials with bitter taste (0.5 mM quinine), 20 trials with sweet taste (4 mM AceK). To examine the effect of amygdalar nuclei on taste preference, 50% of sweet trials in Fig. 4c or 50% of bitter trials in Fig. 4e were pseudo-randomly coupled to photostimulation of the CEA (Fig. 4c) or BLA (Fig. 4e). The delivery of tastants was triggered by licking actions such that mice could consume as much or little as they chose during the 5 s. To minimize the influence of thirst and satiety on the assessment of taste palatability, for each test session in Fig. 4 we included consecutive trials satisfying two criteria: (1) licks to bitter less than 20 (otherwise mice were too thirsty); (2) more than 5 licks to water (otherwise mice were already satiated). The licking behaviour was videotaped during the entire session and licking events were identified by a custom-written code in MATLAB. For photostimulation, 473-nm light stimuli (diode-pumped solid-state laser, Shanghai Laser & Optics Century Co. or fibre-coupled LED, Thorlabs) were delivered via an optical fibre inserted into a guide cannula over the amygdala or via an implantable fibre over the taste cortex. Light stimulation was controlled by contact of the tongue with the metal spout; one lick triggered a train of light pulses (10–20 Hz, 20 ms per pulse, 20 pulses, 5–15 mW per mm²). Licks during the light stimulation extended the stimulus until 1 s after the last lick. Light/tone cues, the delivery of tastants and light stimuli were controlled using a MATLAB program via a microcontroller board (Arduino Mega 2560, Arduino)⁷. Each point in Fig. 3c–f and Fig. 4 indicates data averaged from multiple test sessions for an individual mouse. In Fig. 3e, f, the lick ratio refers to the number of licks in the presence of light stimulation over the number of licks in water-only trials.

Free-moving lick preference assays. Taste preference (Fig. 5g–i) was also measured in free-moving animals by using a custom-built gustometer³³. Prior to testing, mice were water-restricted for 24 h, and then provided with water until they exhibited an average of <20 licks per 5-s window (to test attractive responses). Alternatively, after 24 h of water-restriction mice were provided with unrestricted water access for 5–10 min, and then assayed 18 h later (that is, to test aversive responses animals need to be sufficiently thirsty to be motivated to sample an unattractive cue). For testing, mice were presented with water versus 4 mM AceK or water versus 1 mM quinine as previously described³³.

Place-preference assays. Mice expressing Chr2 in sweet or bitter cortex were tested in a custom-built two-chamber arena placed inside a sound-attenuating cubicle; the arena (30 cm × 15 cm), was designed with two chambers, one with alternating black and white vertical stripes, and the other with alternating black and white squares. Animal locations were tracked in real-time by videotaping⁷. Mice were tested in the arena for 30 min with photostimulation of the sweet or bitter cortico-amygdalar projections via an optical fibre above the BLA or CEA, respectively. The last 15 min of each testing session was used to calculate the preference index (PI); $PI = (t_1 - t_2)/(t_1 + t_2)$, where t_1 is the fraction of time a mouse spent in the chamber 1 (stimulating chamber), and t_2 is the time spent in chamber 2 (non-stimulating chamber). For photostimulation of the sweet cortico-amygdalar projections, light was delivered for 5 s, with a 3-s interval (20 Hz, 20-ms pulses, 5–10 mW per mm²) to avoid over-stimulation or phototoxicity; for photostimulation of the bitter cortico-amygdalar projection, light (20 Hz, 20-ms pulses, 2–5 mW per mm²) was delivered for 1 s with a 3-s interval; a sound cue was used to mark the onset of each stimulation^{15,34,35}. For each cohort (8 mice for sweet and 5 animals for bitter), half the animals were tested with light on in the baseline-preferred chamber, and half with light on in the baseline-unpreferred chamber^{15,34}. When the mouse crossed to the non-stimulating chamber, the light was automatically turned off immediately.

Three-port taste-recognition assays. Mice deprived of water for 24 h were trained to perform a taste-recognition task in a customized three-port behaviour chamber in which they sampled taste cues from the middle port and then reported the taste identity of the cue by choosing to lick from either the left or right port. Taste cues (AceK, quinine or water) were pseudo-randomly delivered through a metal spout in the middle port. Each trial began with the shutter opening in the middle port. Mice were given (up to) 15 s to initiate a trial by licking the middle spout (failure to initiate a trial resulted in the shutter closing and a new trial starting). The shutter in the middle port closed 0.5 s after the first lick allowing animals 0.5 s to sample tastants cues (2–3 μ l); 0.5 s after the middle port closed, the shutters of the left and right ports opened simultaneously. Mice were given 4 s to make a left or right choice and obtain the water reward (total ~6 μ l). For a given mouse, reward from side ports was assigned to taste cues (for example, left for sweet, right for bitter and water). A wrong choice triggered a penalty of a 5-s timeout. The inter-trial interval was 1 s. Mice were trained for two sessions per day, with 80–100 pseudo-randomized trials per session until they could effectively discriminate the tastants with approximately 90% accuracy (2–3 weeks). To test the effect of photostimulation of sweet cortical neurons, mice expressing Chr2 in the sweet cortex were trained to discriminate sweet from bitter and water (for example, left for sweet, right for either bitter or water) and then tested with sweet, bitter, water and water with light (473 nm, 20 Hz, 20 ms per pulse, 20 pulses triggered by one lick of the middle spout). A testing session consisted of 20 sweet trials, 20 bitter trials, 10 water-only trials and 10 water with light trials. To avoid mice using photostimulation light as a visual cue, the connection between implantable fibre and patch cable was properly shielded. To prevent learning during the test, no time-out penalties were given and no reward was provided for water with light trials. Performances were calculated as the percentage of correct choices for a given taste cue. The lick behaviour was detected by a capacitive touch sensor (MPR121, SparkFun). The delivery of tastants, shutter position and light stimuli were controlled by a custom-written program in MATLAB via an Arduino board.

Go/no-go taste-recognition assays. Go/No-go taste-recognition assays were performed as previously described⁷. Mice were trained until they could effectively discriminate the tastants with approximately 90% accuracy (over 1–2 weeks).

On the ‘probe’ sessions, no punishment was applied for ‘no-go’ tastants to avoid re-learning; neither reward nor punishment were delivered to novel tastants.

Pharmacological inhibition. The selective AMPA receptor antagonist NBQX (2,3-dioxo-6-nitro-1,2,3,4-tetrahydrobenzo[*f*]quinoxaline-7-sulfonamide, 5 mg ml⁻¹ in 0.9% NaCl, 100–300 nl, Tocris Bioscience) was unilaterally (Fig. 3e, f) or bilaterally (Figs. 5, 6) infused into the amygdala using a 1- μ l microsyringe (Hamilton) and an internal cannula (PlasticsOne) inserted into the guide cannula above the amygdala. The infusion rate was approximately 100 nl min⁻¹. After intracranial infusion, mice were allowed to rest in their home cage for 1–1.5 h before re-test. A post-test was performed after a recovery period of 24 h. As a control, the same experiment was conducted using isotonic saline (0.9% NaCl) in the same animals.

Chemogenetic inhibition. Mice injected with Chr2 in the sweet cortex and hM4Di in the BLA were first tested in the head-restrained lick preference assay as described above. To effectively examine inhibition using hM4Di, we determined (and used) the minimum light intensity for photostimulation that produced significant attractive responses (pre-test). On the following day, CNO was injected (10 mg kg⁻¹, intraperitoneal) and the behavioural test with the same level of photostimulation was repeated between 1 and 2 h after CNO injection. Mice were allowed to rest and recover in their home cage and a post-test was performed at least 24 h later.

The same mice were then trained in the three-port assay for taste recognition. After achieving at least 90% accuracy in training sessions, mice were tested for the ability to recognize tastants and optogenetic stimulation of the sweet cortex in the three-port taste-recognition assay before and after chemogenetic silencing (pre: 24 h before CNO injection; CNO: between 1–2 h after injection; post: at least 24 h after injection). To confirm that amygdala was indeed efficiently silenced in the experiments presented in Fig. 6c, mice were tested for attractive responses to photostimulation of the sweet cortex in a lick preference assay; this was performed after each three-port session before and after chemogenetic silencing.

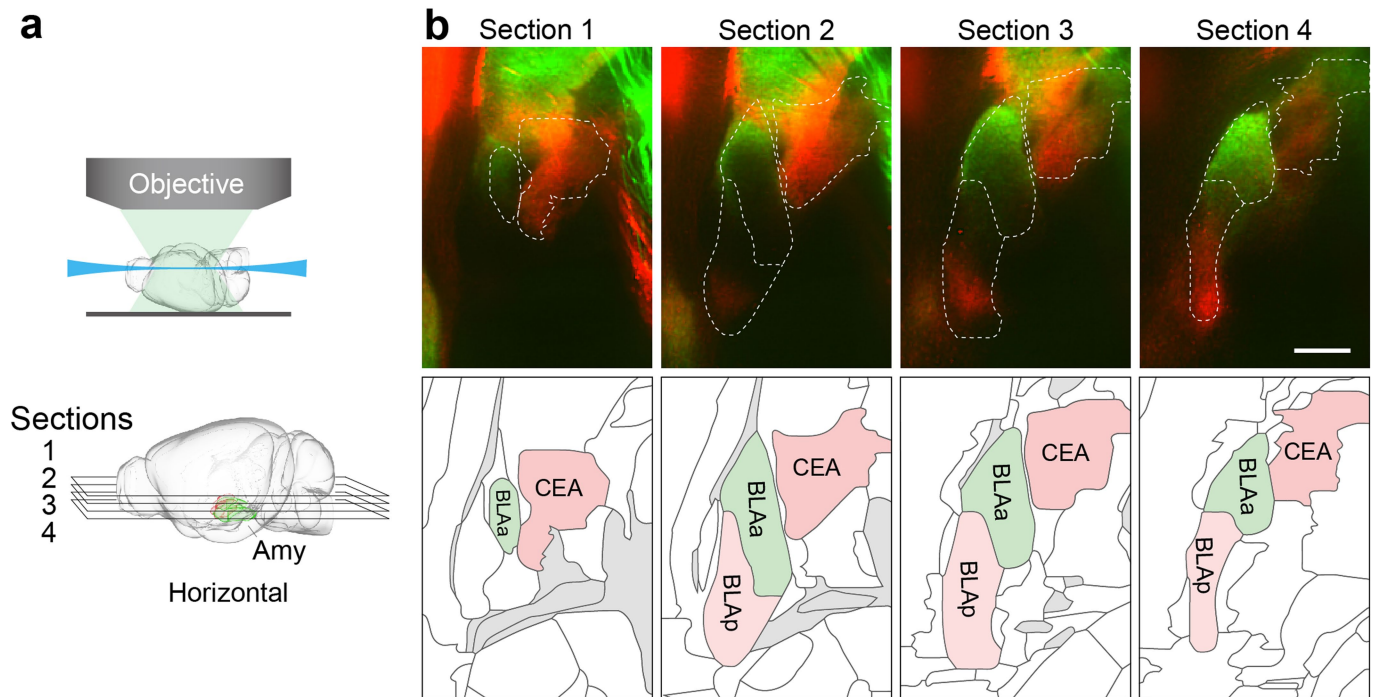
Statistics. No statistical methods were used to predetermine sample size, and investigators were not blinded to group allocation. No method of randomization was used to determine how animals were allocated to experimental groups. Animals in which post hoc histological examination showed that viral targeting or the position of implanted fibre/cannulas was in the wrong location were excluded from analysis. Statistical methods are indicated when used, and statistical analyses for all figures are provided in Supplementary Table 1. Multiple comparisons were analysed using repeated-measures one-way or two-way ANOVAs followed by the Bonferroni correction. All analyses were performed in MATLAB 2016a (MathWorks), Prism 7.0a (GraphPad) and Igor Pro 6.37 (WaveMetrics). Data are presented as mean \pm s.e.m.

Reporting summary. Further information on experimental design is available in the Nature Research Reporting Summary linked to this paper.

Code availability. Custom code for behavioural assays is available from the corresponding author upon reasonable request.

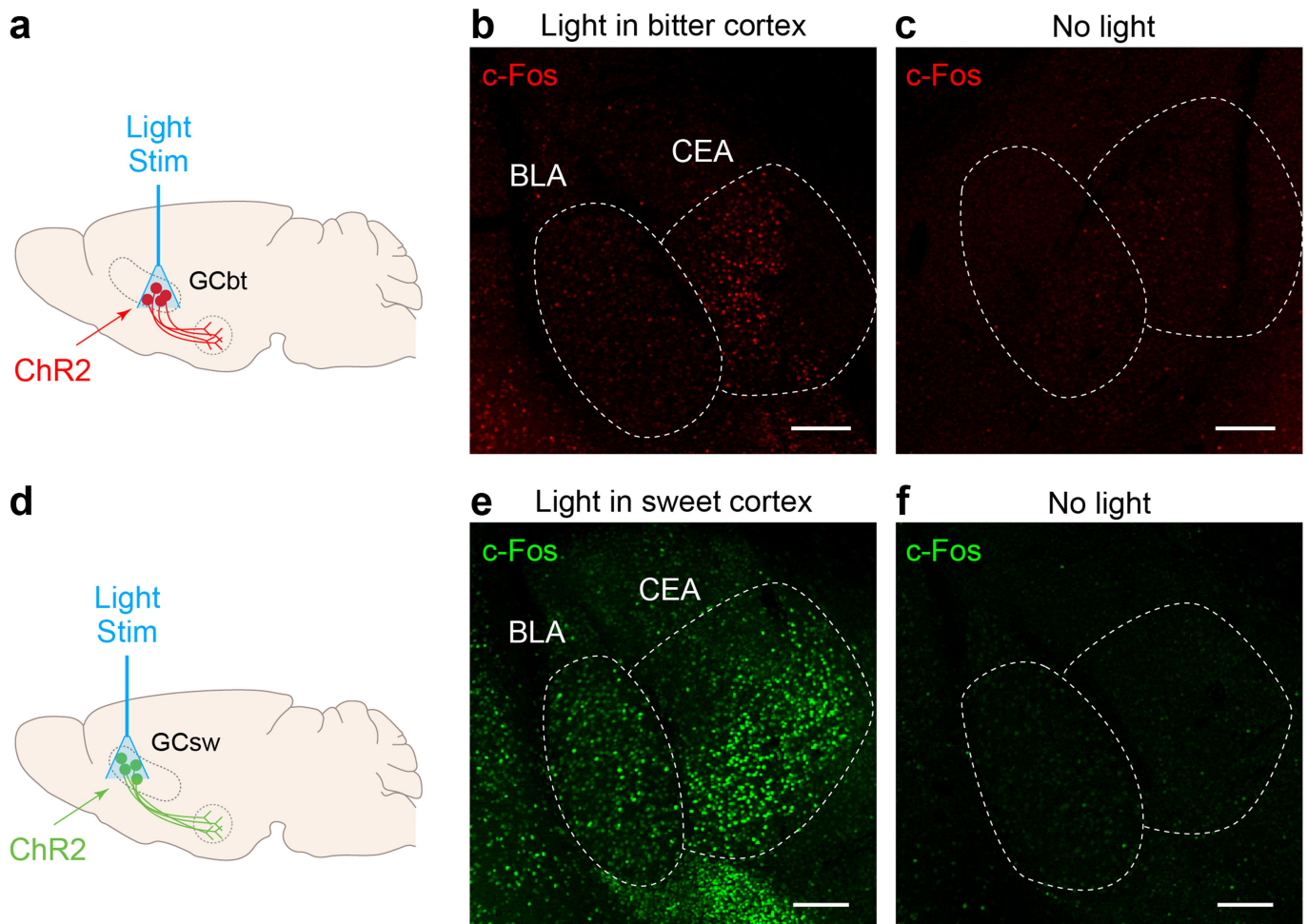
Data availability. All data supporting the findings of this study are available from the corresponding author upon reasonable request.

- Madisen, L. et al. A robust and high-throughput Cre reporting and characterization system for the whole mouse brain. *Nat. Neurosci.* **13**, 133–140 (2010).
- Sasaki, E. A. et al. Advanced CUBIC protocols for whole-brain and whole-body clearing and imaging. *Nat. Protoc.* **10**, 1709–1727 (2015).
- Avants, B. B. et al. A reproducible evaluation of ANTs similarity metric performance in brain image registration. *Neuroimage* **54**, 2033–2044 (2011).
- Zhang, Y. et al. Coding of sweet, bitter, and umami tastes: different receptor cells sharing similar signaling pathways. *Cell* **112**, 293–301 (2003).
- Kim, C. K. et al. Molecular and circuit-dynamical identification of top-down neural mechanisms for restraint of reward seeking. *Cell* **170**, 1013–1027 (2017).
- Illango, A. et al. Similar roles of substantia nigra and ventral tegmental dopamine neurons in reward and aversion. *J. Neurosci.* **34**, 817–822 (2014).
- Krettek, J. E. & Price, J. L. A description of the amygdaloid complex in the rat and cat with observations on intra-amygdaloid axonal connections. *J. Comp. Neurol.* **178**, 255–279 (1978).



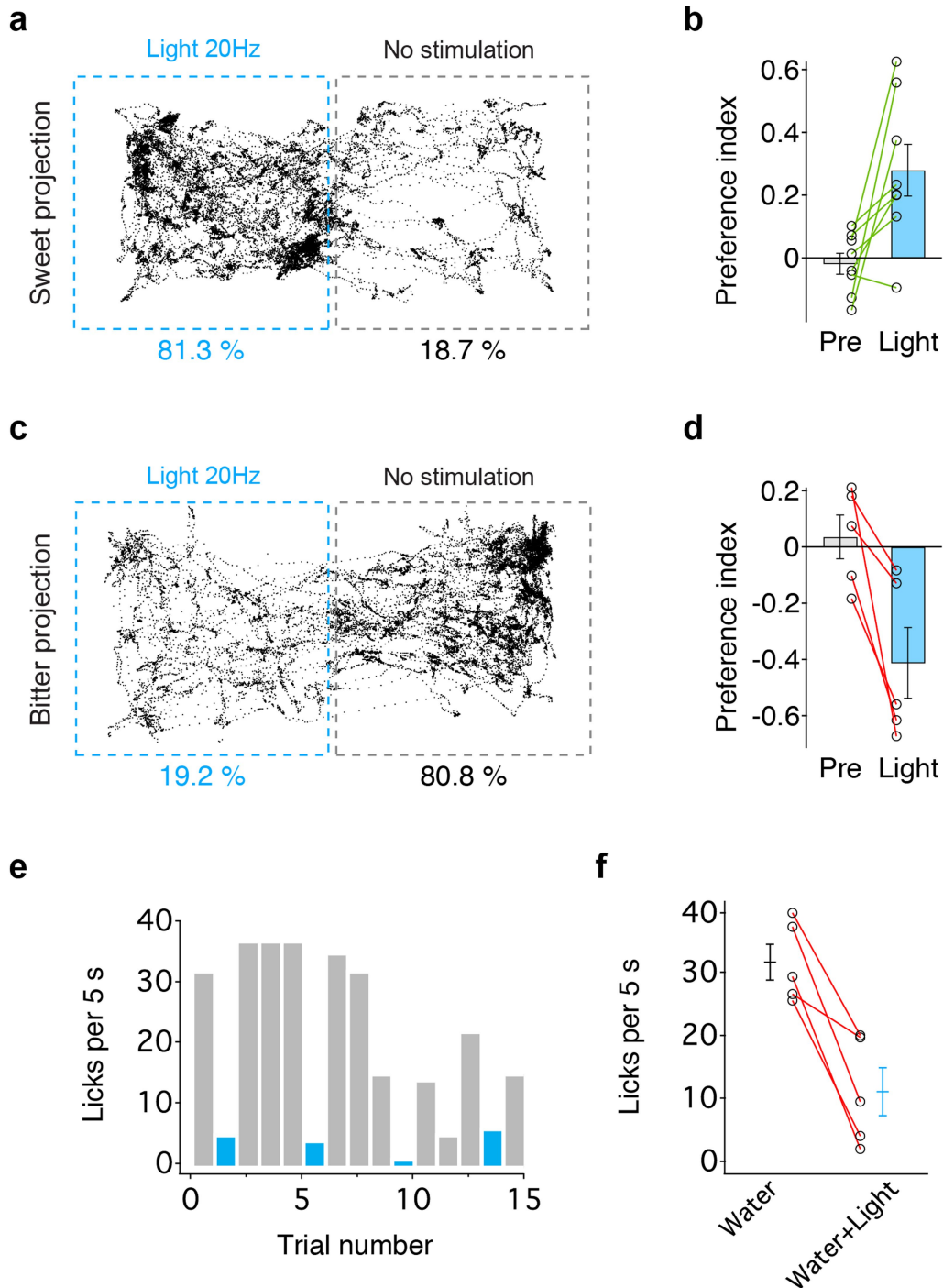
Extended Data Fig. 1 | Projections from the sweet and the bitter cortex terminate in distinct targets in the amygdala. **a**, The cartoon illustrates the imaging planes of the optical horizontal sections at different depths of the amygdala. The brain diagrams were rendered by the scalable brain composer (https://scalablebrainatlas.incf.org/services/sba-composer.php?template=ABA_v3) based on the Allen Mouse Brain Common Coordinate Framework version 3^{26,27}. **b**, Segregation of sweet and bitter cortical projections in the amygdala. Sweet cortical neurons project to

anterior BLA (green), whereas bitter cortical neurons predominantly innervate the CEA (red) and a portion of the posterior BLA (red). Top, optical horizontal sections at different dorsal–ventral positions are shown (sections 1–4; see **a**). Bottom, the boundaries of amygdala nuclei were determined by aligning fluorescence images to the Allen Brain Institute atlas²⁶ (<http://brain-map.org/>). Scale bar, 500 μm . Similar results were observed in six independently labelled and imaged animals.



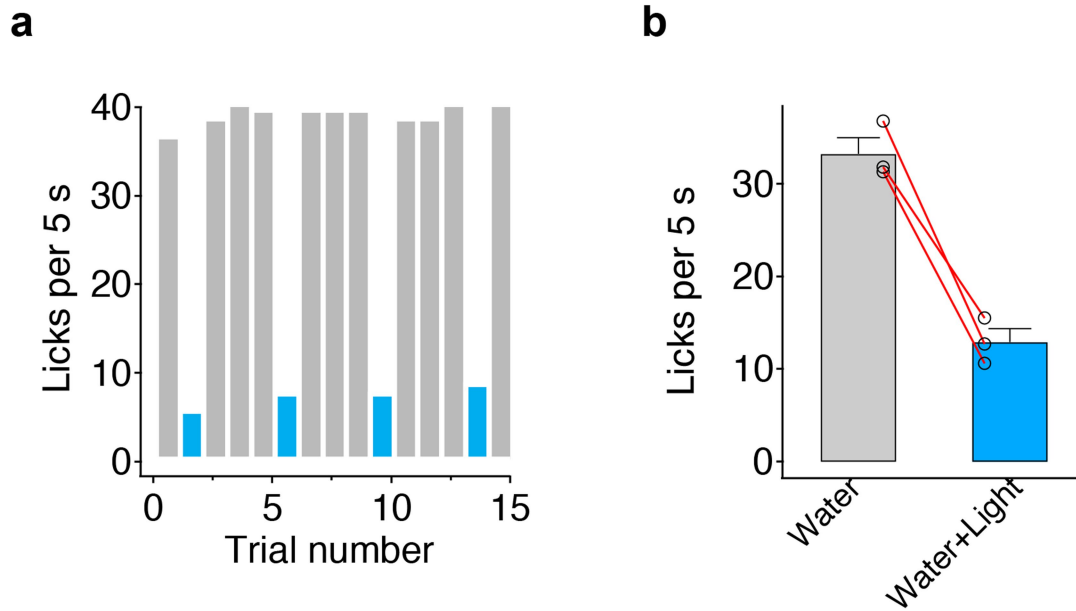
Extended Data Fig. 2 | Activity-dependent labelling of sweet and bitter cortical targets in the amygdala. Fos expression¹⁶ in response to optogenetic activation of the sweet and bitter cortical fields was used to label activated neurons. **a**, Schematic of optogenetic stimulation strategy in the bitter cortex for Fos induction. **b**, Fos expression in the amygdala in response to photostimulation of the bitter cortex. The majority of Fos⁺

neurons are localized in the CEA. **c**, Fos expression in a control mouse without light stimulation. **d–f**, Photostimulation of the sweet cortex induces Fos expression in the amygdala. Note that the CEA, as a major local output of the BLA^{11,36}, also shows strong Fos labelling in response to photostimulation. Scale bars, 200 μ m. Similar results were obtained in three animals for each experiment.



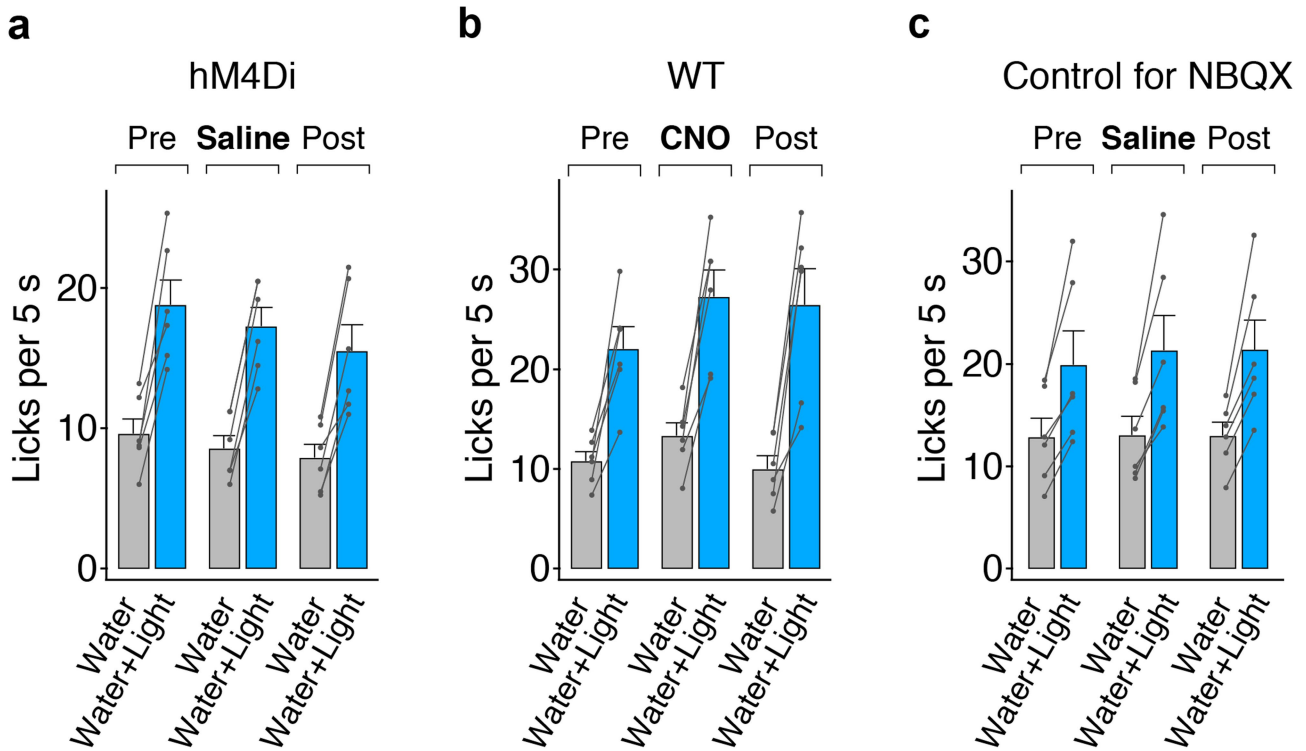
Extended Data Fig. 3 | Place preference by photostimulation of cortico-amygdalar projections. **a**, Representative tracking of a mouse during the 15-min place-preference test in a two-chamber arena; the left chamber in the diagram was coupled to stimulation of sweet cortico-amygdalar projections (see Methods for details); this animal spent over 80% of the test time in the chamber linked to stimulation of sweet projections to the amygdala. **b**, Quantification of preference index before (Pre) and during light stimulation. $n = 8$ mice, two-tailed paired t -test, $P = 0.0156$. **c**, **d**, Place-preference test with stimulation of bitter cortical projections in the amygdala. $n = 5$ mice, two-tailed paired t -test, $P = 0.0207$. **e**, **f**, Animals

used in **d** were also tested in a licking assay with similar light stimulation intensity, demonstrating strong suppression of licking responses. $n = 5$ mice, two-tailed paired t -test, $P = 0.0056$. Values are mean \pm s.e.m. We note that we have examined multiple independent behavioural experiments activating sweet projections to the BLA and have never observed the induction of motor patterns or consummatory behaviour. Strong stimulation of bitter cortico-amygdalar projections (20 Hz, 10–15 mW) often elicited prototypical orofacial rejection behaviour (Supplementary Video 1).



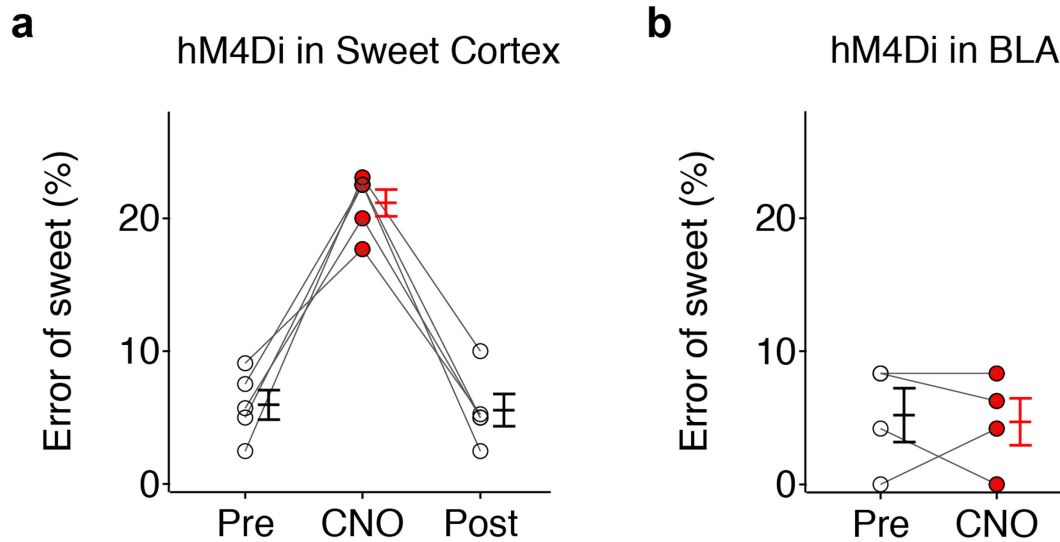
Extended Data Fig. 4 | Activation of bitter cortical projections to posterior BLA is aversive. As shown in Fig. 1 and Extended Data Fig. 1, a fraction of the bitter cortico-amygdalar projections terminate in the posterior BLA. As expected, stimulation of these projections elicits aversive responses. **a**, Representative histograms showing licking events in the presence (blue) or absence (grey) of photostimulation of bitter cortical

projections to the posterior BLA. AAV-ChR2 was injected into the bitter cortex, and the stimulating fibre was targeted above the posterior BLA (coordinates: bregma -2 mm; lateral 3.4 mm; ventral 4.3 mm). **b**, Quantification of licking responses. $n = 3$ mice, two-tailed paired t -test, $P = 0.0121$. Values are mean \pm s.e.m.



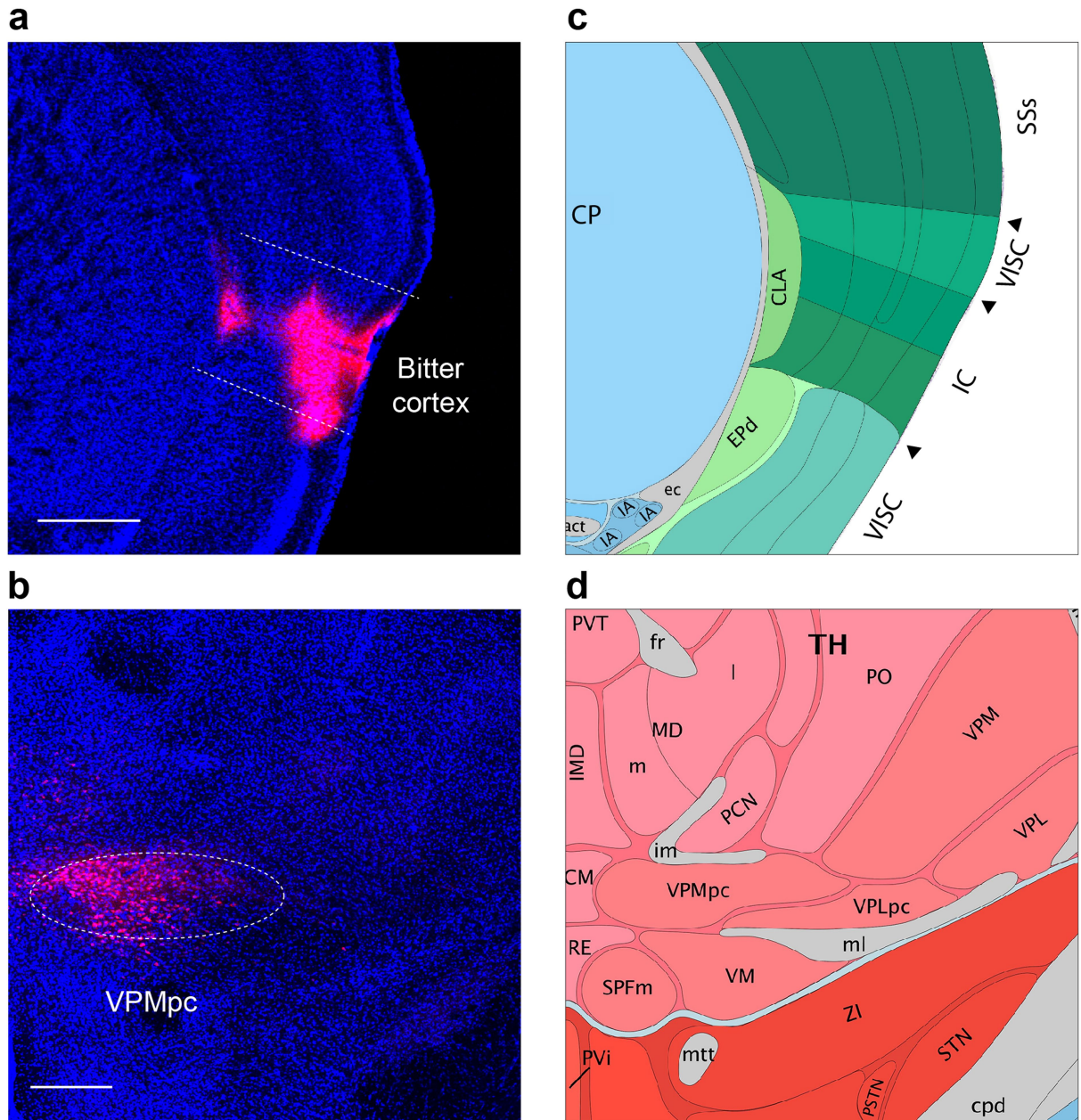
Extended Data Fig. 5 | Control experiments for silencing amygdala with DREADD and NBQX. a, Quantification of licking response before and after saline administration in mice that expressed inhibitory DREADD (hM4Di; see Fig. 5). $n = 6$ mice, two-tailed paired t -test; pre, $P = 0.0011$; saline, $P < 0.0001$; post, $P = 0.0014$. **b,** Quantification of licking response before and after CNO administration (10 mg kg^{-1}) in wild-type (WT)

non-DREADD-expressing animals. $n = 6$ mice, two-tailed paired t -test; pre, $P = 0.0025$; CNO, $P = 0.0008$; post, $P = 0.0021$. **c,** Controls with saline infusion instead of NBQX for Fig. 5c. $n = 6$ mice, two-tailed paired t -test; pre, $P = 0.0080$; saline, $P = 0.0054$; post, $P = 0.0046$. Values are mean \pm s.e.m.



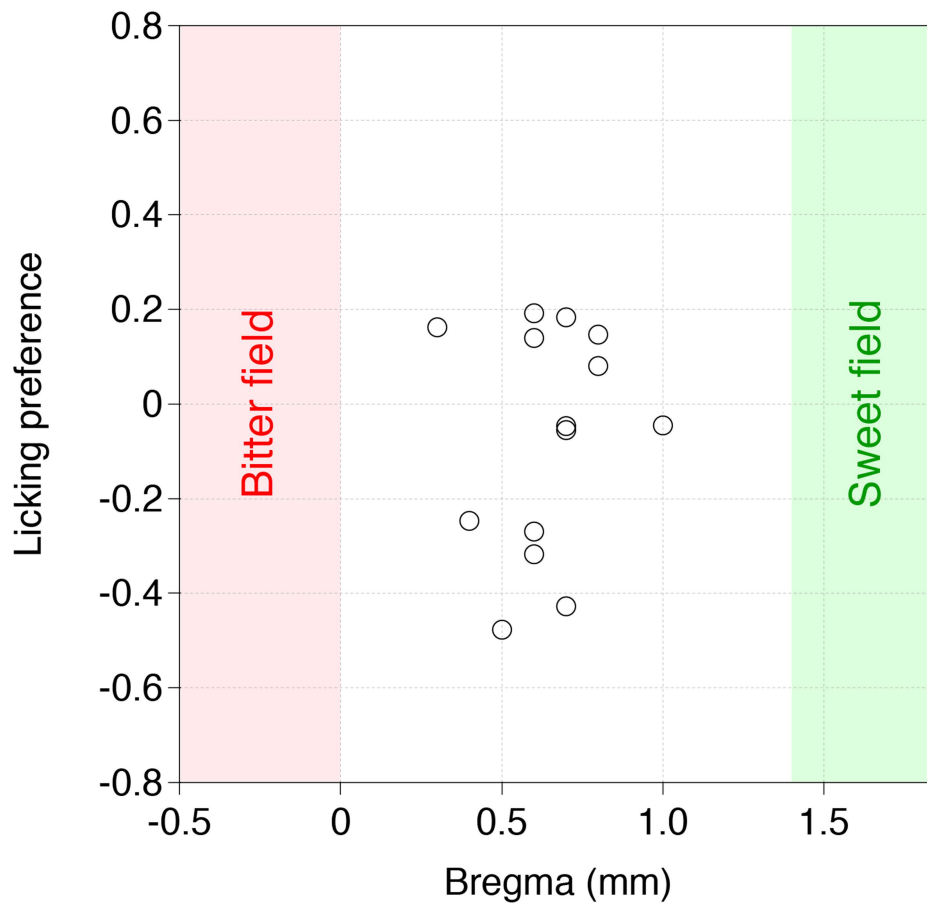
Extended Data Fig. 6 | Chemogenetic silencing of neurons in the taste cortex impairs tastant recognition. **a**, Quantification of the error rate for sweet taste recognition (2 mM AceK) in a three-port assay before and after silencing neurons in the sweet taste cortex with inhibitory DREADD (hM4Di) and CNO (10 mg kg⁻¹). $n = 5$ mice, repeated-measures one-way ANOVA followed by Bonferroni post hoc test, $F_{2,8} = 46.84$, $P < 0.0001$. Pharmacological silencing data using NBQX can be found in a previously published study⁷. **b**, Quantification of the error rate of sweet taste

recognition (1 mM AceK) before and after silencing of the amygdala with inhibitory DREADD (hM4Di) and CNO (10 mg kg⁻¹). $n = 4$ mice, two-tailed paired t -test; pre versus CNO, $P = 0.7888$. See also Fig. 6. Note that sweet recognition was only affected by silencing the taste cortex, but not the amygdala. All tested animals recognized sweet taste with the correct behavioural choice (before silencing) in at least 90% of the trials. Values are mean \pm s.e.m. See Supplementary Table 1 for detailed statistics.



Extended Data Fig. 7 | Retrograde labelling of gustatory thalamic neurons. a, b, Injection of the retrograde tracer cholera toxin subunit B–Alexa Fluor 594 in the taste cortex (bitter cortical field; shown in red in a)

selectively labels neurons in the taste thalamus (VPMpc; b). Similar results were observed in two animals. **c, d,** Diagrams of the corresponding brain regions, adapted from the Allen Brain Institute atlas. Scale bars, 500 μ m.



Extended Data Fig. 8 | Licking responses to photostimulation of intermediate regions between sweet and bitter cortex. Behavioural responses (see Fig. 3) in water-only trials linked to contact-driven self-stimulation are shown for mice expressing ChR2 between the sweet and

bitter cortical fields. Note that a positive index means attraction, whereas a negative index means aversion to light stimulation. $n = 14$ mice. Data points indicate the behavioural test of individual animals at different stimulation sites relative to bregma position.

Reporting Summary

Nature Research wishes to improve the reproducibility of the work that we publish. This form provides structure for consistency and transparency in reporting. For further information on Nature Research policies, see [Authors & Referees](#) and the [Editorial Policy Checklist](#).

Statistical parameters

When statistical analyses are reported, confirm that the following items are present in the relevant location (e.g. figure legend, table legend, main text, or Methods section).

n/a Confirmed

- The exact sample size (n) for each experimental group/condition, given as a discrete number and unit of measurement
- An indication of whether measurements were taken from distinct samples or whether the same sample was measured repeatedly
- The statistical test(s) used AND whether they are one- or two-sided
Only common tests should be described solely by name; describe more complex techniques in the Methods section.
- A description of all covariates tested
- A description of any assumptions or corrections, such as tests of normality and adjustment for multiple comparisons
- A full description of the statistics including central tendency (e.g. means) or other basic estimates (e.g. regression coefficient) AND variation (e.g. standard deviation) or associated estimates of uncertainty (e.g. confidence intervals)
- For null hypothesis testing, the test statistic (e.g. F , t , r) with confidence intervals, effect sizes, degrees of freedom and P value noted
Give P values as exact values whenever suitable.
- For Bayesian analysis, information on the choice of priors and Markov chain Monte Carlo settings
- For hierarchical and complex designs, identification of the appropriate level for tests and full reporting of outcomes
- Estimates of effect sizes (e.g. Cohen's d , Pearson's r), indicating how they were calculated
- Clearly defined error bars
State explicitly what error bars represent (e.g. SD, SE, CI)

Our web collection on [statistics for biologists](#) may be useful.

Software and code

Policy information about [availability of computer code](#)

Data collection

Custom MATLAB programs and Arduino codes were used to drive hardware and collect data in the behavioral experiments. The MATLAB program used in the head-restrained licking preference tests was as described by Peng, Y. et al. Nature 527, 512-515, (2015). All custom MATLAB programs and Arduino code are available upon request.

Data analysis

ImageJ 1.51n and Advanced Normalization Tools 1.91x were used to analyze imaging data. MATLAB 2016a, Igor Pro 6.37 and Prism 7.0a were used in statistic analysis.

For manuscripts utilizing custom algorithms or software that are central to the research but not yet described in published literature, software must be made available to editors/reviewers upon request. We strongly encourage code deposition in a community repository (e.g. GitHub). See the Nature Research [guidelines for submitting code & software](#) for further information.

Data

Policy information about [availability of data](#)

All manuscripts must include a [data availability statement](#). This statement should provide the following information, where applicable:

- Accession codes, unique identifiers, or web links for publicly available datasets
- A list of figures that have associated raw data
- A description of any restrictions on data availability

All data supporting the findings of this study are available upon request.

Field-specific reporting

Please select the best fit for your research. If you are not sure, read the appropriate sections before making your selection.

Life sciences Behavioural & social sciences

For a reference copy of the document with all sections, see nature.com/authors/policies/ReportingSummary-flat.pdf

Life sciences

Study design

All studies must disclose on these points even when the disclosure is negative.

Sample size	No statistical methods were used to calculate the sample size. Sample size was determined based on our experience and the sample size used in similar studies.
Data exclusions	Animals in which post-hoc histological examination showed that viral targeting or the position of implanted fiber / cannulas were in the incorrect location were excluded from analysis.
Replication	All attempts at replication were successful.
Randomization	Stimuli were presented in random order (as described in the manuscript), otherwise no randomization was used.
Blinding	Investigators were not blinded to group allocation.

Materials & experimental systems

Policy information about [availability of materials](#)

n/a	Involvement in the study
<input checked="" type="checkbox"/>	<input type="checkbox"/> Unique materials
<input type="checkbox"/>	<input checked="" type="checkbox"/> Antibodies
<input checked="" type="checkbox"/>	<input type="checkbox"/> Eukaryotic cell lines
<input type="checkbox"/>	<input checked="" type="checkbox"/> Research animals
<input checked="" type="checkbox"/>	<input type="checkbox"/> Human research participants

Antibodies

Antibodies used	Goat anti-c-Fos antibody (Santa Cruz, sc-52-G), Lot: I0315, 200ug/ml, 1:500.
Validation	Goat anti-c-Fos antibody (Santa Cruz, sc-52-G) has been validated extensively, eg, by immunostaining on mouse brain sections (Choi, et al. Cell, 146, 1004-1015, (2011)).

Research animals

Policy information about [studies involving animals](#); [ARRIVE guidelines](#) recommended for reporting animal research

Animals/animal-derived materials	Mus musculus, C57BL/6J and B6.Cg-Gt(ROSA)26Sortm9(CAG-tdTomato)Hze/J male mice were used. All animals used were younger than 8 months old. When performing viral injections, we generally used 7-9 weeks old animals.
----------------------------------	---

Method-specific reporting

n/a	Involvement in the study
<input checked="" type="checkbox"/>	<input type="checkbox"/> CHIP-seq
<input checked="" type="checkbox"/>	<input type="checkbox"/> Flow cytometry
<input checked="" type="checkbox"/>	<input type="checkbox"/> Magnetic resonance imaging